

Synthesis and optical properties of germanium nanorod array fabricated on porous anodic alumina and Si-based templates

Y. F. Mei^{a)}

Department of Physics and Materials Science, City University of Hong Kong, Tat Chee Avenue, Kowloon, Hong Kong, China

Z. M. Li,^{b)} R. M. Chu, and Z. K. Tang

Department of Physics, Hong Kong University of Science and Technology, Clear Water Bay, Kowloon, Hong Kong, China

G. G. Siu, Ricky K. Y. Fu, and Paul K. Chu

Department of Physics and Materials Science, City University of Hong Kong, Tat Chee Avenue, Kowloon, Hong Kong, China

W. W. Wu and K. W. Cheah

Department of Physics, Hong Kong Baptist University, Kowloon, Hong Kong, China

(Received 18 August 2004; accepted 10 November 2004; published online 5 January 2005)

A large quantity of monocrystalline germanium nanorods and their arrays were produced on a porous anodic alumina (PAA) template utilizing saturated vapor adsorption, during which the Ge gas pressure was saturated at a high temperature in an airtight quartz tube. Raman scattering and photoluminescence (PL) results were acquired from the Ge nanorod array and discussed in details. Using Si-based PAA template with 25 nm nanopores, Si-based Ge nanorod array with a large area (larger than $1 \times 1 \text{ cm}^2$) was obtained and the quantum confinement effect is demonstrated in Raman spectrum. © 2005 American Institute of Physics. [DOI: 10.1063/1.1849854]

Because of quantum confinement in the circumferential direction, one-dimensional nanomaterials exhibit interesting properties.¹ Nanowires and nanorods of different compositions have been fabricated by various methods such as chemical vapor deposition,^{2,3} laser ablation,⁴ and thermal evaporation.^{5,6} More recently, the oriented arrays consisting of nanomaterials, such as diamond nanocylinder,⁷ iron nanorod,⁸ single-crystal bismuth nanowire,⁹ and indium-oxide nanowire,¹⁰ have also been synthesized through carefully designed growth process, and they have advanced the application of nanomaterials.¹ However, with the exception of individual nanowires or rods, the synthesis of large-area arrays of silicon or germanium nanorods has not been explored too much because of the complicated growth mechanism, especially on Si substrate.^{2-6,11}

In this letter, a large quantity of monocrystalline germanium nanorods and their array were produced on a porous anodic alumina (PAA) template utilizing saturated vapor adsorption, during which the Ge gas pressure was saturated at a high temperature in an airtight quartz tube. Raman scattering and photoluminescence (PL) spectra were measured and analyzed on the fabricated Ge nanorod array. Using a Si-based PAA template with 25 nm nanopores, a Ge nanorod array with large area (larger than $1 \times 1 \text{ cm}^2$) was obtained and the quantum confinement is demonstrated in the Raman spectrum.

The PAA template was fabricated by a conventional two-step method.^{12,13} Our fabrication of monocrystalline Ge nanorods was based on a thermal evaporation process. The source materials consisted of a small tablet of Ge and powders of GeO_2 . They were sealed together with the PAA template in a quartz tube under a pressure of 10^{-3} Pa. The Ge

tablet and GeO_2 were mixed and 10 cm away from the PAA template. The sealed quartz tube was then heated uniformly to 1100°C for about 3 h and then remained in vacuum for 10 h during which time the sample cooled. During the heating process, the tube was filled with the autogenous vapor pressure of germanium. It is expected that Ge vapor in the nanochannels of the PAA will form one-dimensional nanomaterials because of the steric confinement.

The prepared sample was taken out by breaking the quartz tube and directly measured by scanning electron microscopy [(SEM) JEOL JSM-6300] without any treatment. Two kinds of samples were prepared for transmission electron microscopy [(TEM) Philips CM20; High-Resolution TEM, JEOL 2010]. The first sample was grinded into powders and held with a carbon-coated specimen grid. The other sample was immersed in a 5 M NaOH solution for several hours. After condensation of the solution containing nanomaterials, the solution was dropped onto the carbon-coated specimen grid. Figure 1(d) is obtained from the sample prepared by the formed method, and Figs. 1(e) and 1(g), and Fig. 3(b) from the latter.

The PAA template with ordered nanopores of about 52 nm was produced by a conventional method.^{12,13} Figure 1(a) shows the SEM image of the bottom surface of PAA template. Nanopores ~ 52 nm in diameter are hexagonally arranged at an interpore distance of ~ 95 nm. The SEM images in Figs. 1(b) and 1(c) reveal that large quantity of Ge nanorods and their arrays are grown on PAA template. These nanorods are 50–90 nm in diameter and several microns in length. It is noted that Ge nanorods and their array can be grown on both sides of the PAA with similar morphologies.

The TEM images of the Ge nanorods are shown in Figs. 1(d) and 1(e). All of them are straight and uniformly distributed. In a typical image of the Ge nanorods cluster shown in Fig. 1(d), the diameter of Ge nanorod is about 50 nm. The straight Ge nanorods were characterized using selected-area

^{a)}Author to whom correspondence should be addressed; electronic mail: meiyongfeng@nju.org.cn, yf.mei@plink.cityu.edu.hk

^{b)}Now is at School of Physics, Peking University, Beijing, China.

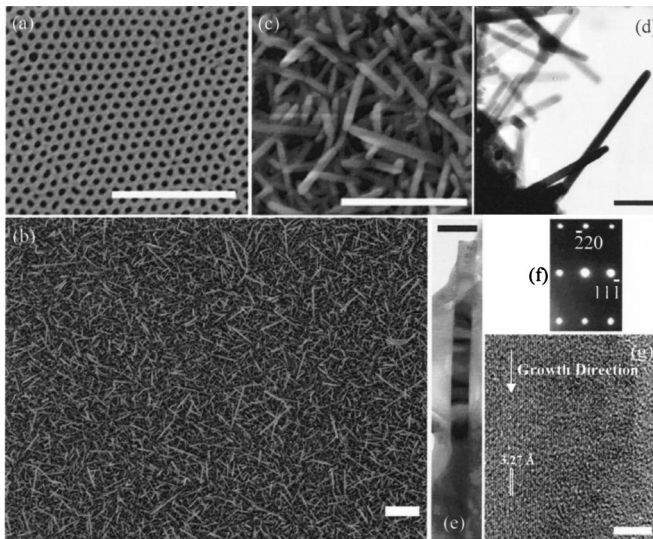


FIG. 1. SEM images of (a) the bottom face of PAA template, (b) the morphology of Ge nanorod array grown on PAA template, and (c) its amplified image; TEM images of (d) Ge nanorod cluster, (e) an individual Ge nanorod and its selected area electron diffraction pattern (f) and high-resolution TEM image (g). [The scale bar: (a), (b), and (c)—1 μm ; (d) and (e)—200 nm; and (g)—5 nm.]

electron diffraction (SAED). The SAED recorded on the nanorod [Fig. 1(e)] exhibits a diffraction pattern [Fig. 1(f)] consistent with the $\langle 112 \rangle$ zone axis of monocrystalline structure of germanium.^{3,5,14} Indexing the pattern further indicates that the Ge nanorods are grown predominantly along the (220) direction. This is confirmed by the high-resolution TEM image in Fig. 1(g) that clearly shows that the atomic lattice with the (111) lattice plane is perpendicular to the wire axis because the spacing between adjacent planes is 3.27 Å and there exists a thin oxide sheath.

Steric confinement by the PAA template is confirmed by Raman scattering spectroscopy performed on our as-prepared sample at room temperature using an excitation wavelength of 514.5 nm on the T64000 Micro-Raman System. A shoulder peak can be clearly observed in Figs. 2(a) and 2(b) on the right-hand side of a main peak at 300 cm^{-1} . The shoulder peak was positioned at 305 cm^{-1} by Gaussian decomposition. Since the excitonic Bohr radius of bulk Ge is 24.3 nm,⁶ which is much smaller than the present Ge nanorods, no quantum confinement effect can be observed in the Ge nanorod array synthesized in PAA template with 50 nm nanopores. Hence, the main peak at 300 cm^{-1} is attributed to the fabricated Ge nanorod. As for the shoulder peak at 305 cm^{-1} , it is the result of a compressive stress effect of the Ge nanorods embedded in the nanopores of the PAA template.^{15–17} In bulk Ge, the transverse optical Raman mode ω_{TO} (cm^{-1}) depends on the pressure p (GPa) as

$$\omega_{\text{TO}} = 300 + 3.85p - 0.039p^2. \quad (1)$$

In a system involving Ge nanocrystals embedded in SiO_2 matrix, a shift of 5 cm^{-1} has been observed and is independent of the crystalline size.¹⁷ This is due to the fact that Ge undergoes a volume expansion of about 6% during the liquid-to-solid phase transition.¹⁸ Since the length of the Ge nanorods is not very long, the case of spherical particles and cavity shape may be adopted for simplification.^{17,19} The compressive stress can be estimated to be 1.4 GPa (p) at the melting temperature (934 °C) of Ge.¹⁷ The effect of the ther-

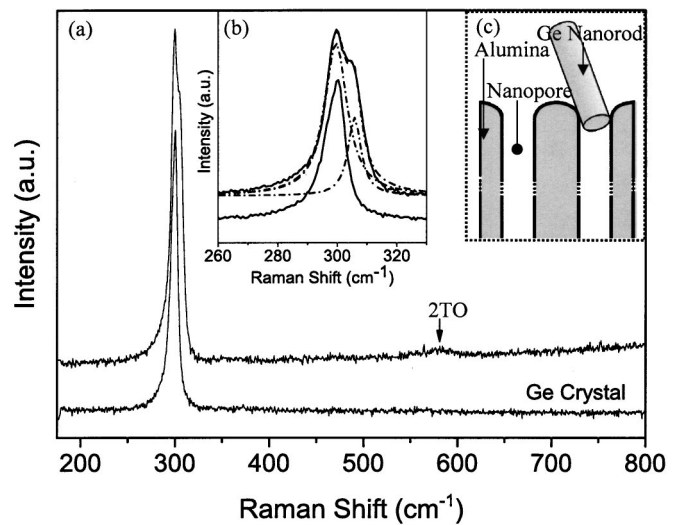


FIG. 2. (a) Raman spectra for Ge nanorod array on PAA template and bulk Ge at room temperature, (b) the fine analysis of Raman bands around 300 cm^{-1} , and (c) a schematic diagram for the structure of Ge nanorod on PAA template.

mal expansion coefficient can be ignored because of the little difference between Ge ($6.1 \times 10^{-6} \text{ K}^{-1}$) and Al_2O_3 ($5.8 \times 10^{-6} \text{ K}^{-1}$). Substituting p into Eq. (1), the Raman frequency is 305.3 cm^{-1} , which is in good agreement with our measured shoulder peak at 305 cm^{-1} . From the above and the schematic diagram of our nanostructures [Fig. 2(c)], we suggest that the main peak comes from the Ge nanorod out of the PAA template, while the shoulder peak originates from the nanorods embedded in the alumina nanopores with the compressive stress effect. Furthermore, it can be deduced that the vapor-liquid-solid (VLS) mechanism contributes to the growth of Ge nanorods on account of the liquid-solid phase transition during growth.¹⁸

The PL property of our sample [Fig. 3(a)] was studied using an excitation wavelength of 325 nm under different temperatures from 300 K to 11 K. A broad peak at 440 nm was observed at 300 K as shown in Fig. 3(a). With the temperature decreasing, another peak at 289 nm was observed at 150 K. A further temperature decrease to 77 K results in increased intensity. At 11 K, there is little enhancement of the PL intensity compared to that observed at 77 K. The broad 440 nm peak shows no change in the PL intensity and can be attributed from the PAA itself as suggested in previous works.¹³ For the 389 nm peak, it is believed to originate from the Ge oxide at the tip of the nanorods as shown in Fig. 3(b). In a system containing Ge oxide, it is commonly accepted that the 290 nm PL peak is related to the transition from the triple state T_1 to the lower single state S_0 at germanium oxygen deficient centers (GODCs).^{20,21} Figure 3(c) depicts a schematic diagram of the energy states of the GODC.²⁰ The single-to-triple transition at 3.7 eV (335 nm) is around at 325 nm (laser), which is a weak transition and can be enhanced at a low temperature. The number of excited electrons from the upper state to T_1 plays a prominent role in the intensity of the PL 3.1 eV (400 nm) when measured at a low temperature.²¹ Hence, by decreasing the temperature, the PL 390 nm peak can be observed in our sample. In addition, Ge oxide exists at the tips of the nanorods, and so an oxide assistant growth (OAG) mechanism also affects the nanorod growth.⁵ X-ray photoelectron spectroscopy results also revealed the existence of Ge oxide (not shown).

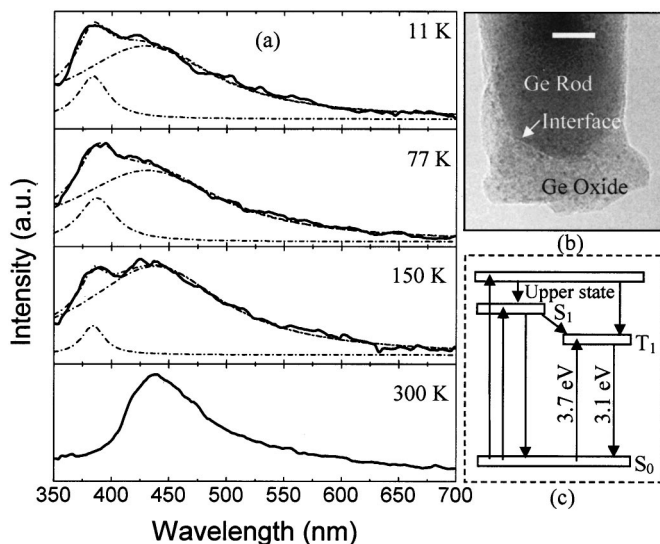


FIG. 3. (a) The PL spectra of Ge nanorod array at different temperatures, (b) a high-resolution TEM image of the Ge nanorod tip (the scale bar: 20 nm), and (c) a schematic diagram of the energy states of the GODC.

As a further application, we applied the Si-based PAA template as the template to fabricate large-area (larger than $1 \times 1 \text{ cm}^2$) and high-quality Ge nanorod arrays. Previously, Si-based PAA templates with nanopores of different sizes were produced using different acids.²² In order to check the quantum confinement effect, a Si-based PAA template with nanopores of 25 nm was adopted. The growth process was similar to the above except that the growth temperature was 900 °C. Figure 4(a) shows the surface morphology of the Ge nanorod array on Si-based PAA template by SEM. An image with large area was shown in Fig. 4(b). Ge nanorods grown from the PAA template stand on it separately [see the cross-section SEM image Fig. 4(c)]. The size of the nanorods is about 15 nm smaller than the excitonic Bohr radius.^{6,23} Therefore, in the Raman scattering measurement [Fig. 4(d)], a shift of about 2 cm^{-1} toward lower frequency is observed for the main peak due to Ge and a similar shoulder peak at 304 cm^{-1} . The former illustrates the behavior of quantum

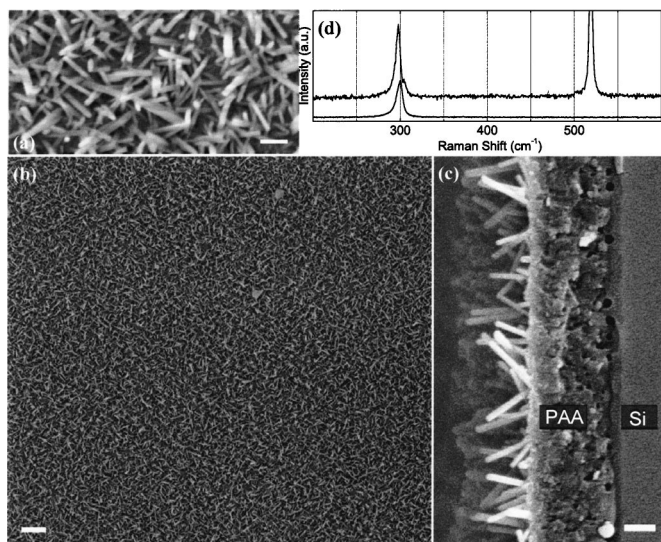


FIG. 4. (a) The SEM image of Ge nanorod array grown on Si-based PAA template with (b) a large-area and (c) its cross-sectional view, (d) Raman spectra for Ge nanorod array on Si-based PAA template (upper) and bulk Ge (lower) at room temperature. [The scale bar: (a) 200 nm, (b) 1 μm , and (c) 200 nm.]

confinement, while the latter is due to the compressive stress as explained before. In its PL spectra (not shown), a peak at $\sim 2 \text{ eV}$ appears compared to that of Ge nanorods with diameter of $\sim 50 \text{ nm}$. Temperature-dependent PL behavior presents a change related to quantum confinement, which will be discussed elsewhere in detail.

In summary, a large quantity of monocrystalline germanium nanorods and their array were produced on a porous anodic alumina (PAA) template. The distinct shoulder peak in the Raman scattering spectrum is due to compressive stress. The PL spectrum obtained at a low temperature shows another peak besides the main peak from the template, which is from the Ge oxide at the tip of the nanorods. Using the Si-based PAA template with 25 nm nanopores, a Si-based Ge nanorod array was successfully synthesized on a large area (larger than $1 \times 1 \text{ cm}^2$) and the quantum confinement is illustrated in the Raman scattering spectrum. The VLS mechanism plays a key role in the formation of nanorods and the OAG mechanism also contributes.

The authors thank M. K. Tang and Dr. Amy X. Y. Lu for experimental assistance. This work was supported by Hong Kong Research Grants Council (RGC) Competitive Earmarked Research Grant (CERG) Nos. CityU1052/02E and CityU1137/03E.

- ¹Y. N. Xia, P. D. Yang, Y. G. Sun, Y. Y. Wu, B. Mayers, B. Gates, Y. D. Yin, F. Kim, and H. Q. Yan, *Adv. Mater. (Weinheim, Ger.)* **15**, 353 (2003), and reference therein.
- ²K. K. Lew, L. Pan, E. C. Dickey, and J. M. Redwing, *Adv. Mater. (Weinheim, Ger.)* **15**, 2073 (2003).
- ³D. W. Wang, and H. J. Dai, *Angew. Chem., Int. Ed.* **41**, 4783 (2002).
- ⁴A. M. Morales, and C. M. Lieber, *Science* **279**, 208 (1998).
- ⁵Y. F. Zhang, Y. H. Tang, N. Wang, C. S. Lee, I. Bello, and S. T. Lee, *Phys. Rev. B* **61**, 4518 (2000).
- ⁶Y. Y. Wu, and P. D. Yang, *Chem. Mater.* **12**, 605 (2000).
- ⁷H. Masuda, T. Yanagishita, K. Yasui, K. Nishio, I. Yagi, T. N. Rao, and A. Fujishima, *Adv. Mater. (Weinheim, Ger.)* **13**, 247 (2001).
- ⁸L. Vayssieres, L. Rabenberg, and A. Manthiram, *Nano Lett.* **2**, 1393 (2002).
- ⁹Z. B. Zhang, X. Z. Sun, M. S. Dresselhaus, and J. Y. Ying, *Phys. Rev. B* **61**, 4850 (2000).
- ¹⁰M. J. Zheng, L. D. Zhang, G. H. Li, X. Y. Zhang, and X. F. Wang, *Appl. Phys. Lett.* **79**, 839 (2001).
- ¹¹N. Wang, Z. K. Tang, G. D. Li, and J. S. Chen, *Nature (London)* **408**, 50 (2000).
- ¹²T. T. Xu, R. D. Piner, and R. S. Ruoff, *Langmuir* **19**, 1443 (2003).
- ¹³H. Masuda and K. Fukuda, *Science* **268**, 1466 (1995); G. S. Huang, X. L. Wu, Y. F. Mei, X. F. Shao, and G. G. Siu, *J. Appl. Phys.* **93**, 582 (2003).
- ¹⁴T. Hanrath and B. A. Korgel, *J. Am. Chem. Soc.* **124**, 1424 (2002).
- ¹⁵D. Olego and M. Cardona, *Phys. Rev. B* **25**, 1151 (1982).
- ¹⁶K. L. Teo, L. Qin, I. M. Noordin, G. Karunasiri, Z. X. Shen, O. G. Schmidt, K. Eberl, and H. J. Queisser, *Phys. Rev. B* **63**, 121306 (2001).
- ¹⁷A. Wellner, V. Paillard, C. Bonafos, H. Coffin, A. Claverie, B. Schmidt, and K. H. Heinig, *J. Appl. Phys.* **94**, 5639 (2003).
- ¹⁸J. Von Borany, R. Grötzschel, K. H. Heinig, A. Markwitz, W. Matz, B. Schmidt, and W. Skorupa, *Appl. Phys. Lett.* **71**, 3215 (1997).
- ¹⁹V. V. Voronkov and R. Falster, *J. Appl. Phys.* **89**, 5965 (2001).
- ²⁰M. Gallagher and U. Österberg, *Appl. Phys. Lett.* **63**, 2987 (1993); J. K. Shen, X. L. Wu, R. K. Yuan, N. Tang, J. P. Zou, Y. F. Mei, C. Tan, and X. M. Bao, and G. G. Siu, *ibid.* **77**, 3134 (2000).
- ²¹M. Fujimaki, Y. Ohki, and H. Nishikawa, *J. Appl. Phys.* **81**, 1042 (1997); M. Gallagher and U. Österberg, *ibid.* **74**, 2771 (1993).
- ²²Y. F. Mei, X. L. Wu, X. F. Shao, G. G. Siu, and X. M. Bao, *Europhys. Lett.* **62**, 595 (2003); Y. F. Mei, G. G. Siu, J. P. Zou, and X. L. Wu, *Phys. Lett. A* **324**, 479 (2004); Y. F. Mei, G. S. Huang, Z. M. Li, G. G. Siu, R. K. Y. Fu, Y. M. Yang, X. L. Wu, Z. K. Tang, and P. K. Chu, *Acta Mater.* **52**, 5633 (2004).
- ²³I. H. Campbell and P. M. Fauchet, *Solid State Commun.* **58**, 739 (1986); X. L. Wu, Y. F. Mei, G. G. Siu, K. L. Wong, K. Moulding, M. J. Stokes, C. L. Fu, and X. M. Bao, *Phys. Rev. Lett.* **86**, 3000 (2001).